Available online at www.sciencedirect.com
SCIENCE DIRECT®
JOURNAL OF COMPUTATIONAL AND APPLIED MATHEMATICS
Journal of Computational and Applied Mathematics 170 (2004) 303–315
www.elsevier.com/locate/cam

On inverse methods for the resolution of the Gibbs phenomenon

R. Pasquetti*

Department of Mathematics, Lab. J.A. Dieudonné, UMR CNRS 6621, Université de Nice-Sophia Antipolis, Parc Valrose, Nice 06108, France

Received 9 July 2003; received in revised form 9 July 2003

Abstract

When Fourier expansions, or more generally spectral methods, are used for the representation of nonsmooth functions, then one has to face the so-called Gibbs phenomenon. Considerable progresses have been made these last years to overcome the Gibbs phenomenon, using direct or inverse approaches, both in the discrete or continuous framework. A discrete inverse method for the global or local reconstruction of a non-smooth function starting from its oscillating (trigonometric) polynomial interpolant is introduced and both its capabilities and limits are emphasized.

Keywords: Gibbs phenomenon; Spectral methods

1. Introduction

It is generally admitted that the use of spectral methods is restricted to the representation of smooth functions, since the "exponential convergence property" gets lost as soon as non-smooth functions are considered (see e.g. [2,3,10] for an introduction to spectral methods). Especially, if discontinuous functions are considered, then the spectral representation is no-longer convergent in the L^∞ norm, due to oscillations at the point of discontinuity. However, in the 1990s attempts have been made to recover a spectrally accurate representation, of a discontinuous periodic function, only starting from its Fourier spectrum [4,7–9]. In contrast with filtering techniques, here the goal is to reconstruct the function with spectral accuracy up to the discontinuity point. The basic idea was to project the oscillating interpolant on ad hoc bases functions defined on sub-intervals where the initial function

* Tel.: +33-492076208; fax: +33-493517974.
E-mail address: rpas@math.unice.fr (R. Pasquetti).

0377-0427/$ - see front matter
doi:10.1016/j.cam.2004.01.026

is smooth. To this end, the Gegenbauer polynomials have been used to satisfy the so-called "Gibbs condition" [7]. Such an approach is direct (explicit), since the Gegenbauer polynomial coefficients are computed explicitly from the Fourier coefficients. Recently, an "inverse method" has been introduced to handle in a straightforward way the same problem [11]. In contrast with the direct approach, this last approach is an inverse one in the sense that the computation of the polynomial expansion coefficients requires the solution of an algebraic linear system. Here we follow the same route, but in a discrete framework, knowing that in practice the reconstruction problem only occurs when the Fourier spectrum is obtained from grid-point values.

The paper is organized as follows: In Section 2 we revisit the method proposed in [11] and then consider the discrete case. In Section 3 we discuss the well-posed feature of the resulting problem and especially focus on the stability property through numerical experiments. Global and local reconstruction procedures are introduced and tested in Section 4. Finally, we conclude in Section 5.

All along the paper we consider the periodic case and use trigonometric polynomials. But the work may be easily extended to different spectral approximations, especially the Lcgendre or Chebyshev polynomials when nonperiodic geometries are considered.

2. Inverse methods for the reconstruction problem

Let $f(x)$ be a 2π-periodic function, bounded, smooth except at a subset of S points, $\{x = y_s\}_{s=1}^{S}$ such that $0 \leqslant y_1 < y_2 < \cdots < y_S < 2\pi$. The problem is to recover a spectrally accurate representation of $f(x)$ from its truncated Fourier spectrum. To this end:

- Let $\{L_i(x)\}_{i\in\mathbb{N}}$ be an orthogonal polynomial basis on the interval $(-1, 1)$, e.g., the Legendre polynomial basis.
- Note: $\bar{y}_s = 0.5(y_s + y_{s-1})$ and $\Delta y_s = y_s - y_{s-1}$ with the convention $y_0 = 0$.
- Introduce the functions

$$L_i^s(x) = \begin{cases} L_i(2(x - \bar{y}_s)/\Delta y_s) & \text{if } x \in [y_{s-1}, y_s], \\ 0 & \text{elsewhere.} \end{cases}$$

Then $f(x)$ may be written as

$$f(x) = \sum_{s=1}^{S} \sum_{i=0}^{\infty} \tilde{f}^s_i L_i^s(x). \tag{1}$$

The main idea is now to start from this equality, in physical space, and then to go in Fourier space, so that the $L_i^s(x)$ and $f(x)$ will be similarly affected by the Gibbs phenomenon.

2.1. Continuous framework

Let us project Eq. (1) onto the basis of the trigonometric polynomials $\{\exp(\mathrm{i}kx)\}_{k\in\mathbb{Z}}$. One obtains

$$\frac{1}{c_k}\int_0^{2\pi} f(x)\exp(-\mathrm{i}kx)\,\mathrm{d}x = \sum_{s=1}^{S}\sum_{i=0}^{\infty} \tilde{f}^s_i \frac{1}{c_k}\int_0^{2\pi} L_i^s(x)\exp(-\mathrm{i}kx)\,\mathrm{d}x, \quad k \in \mathbb{Z},$$

where $i^2 = -1$, $c_k = 2\pi$ if $k = 0$ and $c_k = \pi$ if $k \neq 0$. Then, with $\hat{}$ for denoting the Fourier spectrum:

$$\hat{f}_k = \sum_{s=1}^{S} \sum_{i=1}^{\infty} \tilde{f}^s_i \hat{L}^s_{i,k}. \tag{2}$$

Computation of the $\hat{L}^s_{i,k}$:

$$c_k \hat{L}^s_{i,k} = \int_0^{2\pi} L^s_i(x) \exp(-\mathrm{i}kx)\,\mathrm{d}x = \int_{y_{s-1}}^{y_s} L^s_i(x) \exp(-\mathrm{i}kx)\,\mathrm{d}x$$

so that with $X = 2(x - \bar{y}_s)/\Delta y_s$:

$$c_k \hat{L}^s_{i,k} = \frac{\Delta y_s}{2} \int_{-1}^{1} L_i(X) \exp(-\mathrm{i}k(\Delta y_s X/2 + \bar{y}_s))\,\mathrm{d}X.$$

Assume now that the Fourier and polynomial expansions are truncated consistently, then with $N = \sum_{s=1}^{S} (N_s + 1)$ Eq. (2) yields the complex linear system:

$$\hat{f}_k = \sum_{s=1}^{S} \sum_{i=0}^{N_s} \tilde{g}^s_i \hat{L}^s_{i,k}, \quad 0 \leqslant k \leqslant N/2, \tag{3}$$

where we have assumed N to be even for the sake of simplicity. The $\tilde{g}^s_i$ are coefficients which, once computed, yield the following piecewise polynomial approximation g of f:

$$g(x) = \sum_{s=1}^{S} \sum_{i=0}^{N_s} \tilde{g}^s_i L^s_i(x).$$

Note that Eq. (3) constitutes a system of N real equations for N unknowns because the imaginary part of the $k = 0$ Fourier mode equals 0 for real functions and because, N being even, we disregard the imaginary part of the highest mode.

Of course, if $f(x)$ is piecewise polynomial, of degree $p_s \leqslant N_s$ for $x \in [y_{s-1}, y_s[$, then the reconstruction procedure can be made exact, if the integrals are exactly computed, or at least computed in coherent manner.

2.2. Discrete framework

In practice $f(x)$ is generally only known at some grid points, but the above reconstruction procedure may still be useful.

Let $\{x_j\}_{j=1}^{N_F}$ be the set of points such that $x_j = (j-1)2\pi/N_F$. By discrete Fourier transform (DFT) we compute the spectrum of the trigonometric interpolant of f as a linear combination of the $f(x_j)$:

$$\hat{f}_k = \frac{1}{N_F} \sum_{j=1}^{N_F} f(x_j) \exp(-\mathrm{i}kx_j),$$

where for the sake of simplicity we have kept the notation $\hat{f}_k$. From Eq. (1) we have

$$\sum_{j=1}^{N_F} f(x_j) \exp(-\mathrm{i}kx_j) = \sum_{s=1}^{S} \sum_{i=0}^{\infty} \sum_{j=1}^{N_F} \tilde{f}^s_i L^s_i(x_j) \exp(-\mathrm{i}kx_j)$$

so that one recovers

$$\hat{f}_k = \sum_{s=1}^{S} \sum_{i=0}^{\infty} \tilde{f}^s_i \hat{L}^s_{i,k}, \tag{4}$$

where the $\hat{L}^s_{i,k}$ are now computed by DFT just like the $\hat{f}_k$.

Let us truncate the polynomial expansions. Choosing the N_s such that $N_s + 1 \leqslant N^s_{\mathrm{F}}$, where N^s_{F} is the number of grid-points of the subinterval $[y_{s-1}, y_s[$, then with $N = \sum_{s=1}^{S}(N_s + 1)$ (that again we suppose even without loss of generality) one obtains the complex linear system:

$$\hat{f}_k = \sum_{s=1}^{S} \sum_{i=0}^{N_s} \tilde{g}^s_i \hat{L}^s_{i,k}, \quad 0 \leqslant k \leqslant N/2, \tag{5}$$

which, as in the continuous frame, yields a piecewise polynomial approximation g of f:

$$g(x) = \sum_{s=1}^{S} \sum_{i=0}^{N_s} \tilde{g}^s_i L^s_i(x).$$

Again, if $f(x)$ is piecewise polynomial, of degree p_s for $x \in [y_{s-1}, y_s[$ such that $p_s \leqslant N_s$ then the reconstruction procedure is exact.

As in the continuous frame, Eq. (5) constitutes a system of N real equations for N unknowns, say $A\tilde{\boldsymbol{g}} = \hat{\boldsymbol{f}}$. The fact that we do not consider the imaginary part of the highest mode allows us to support the extreme case $N = N_{\mathrm{F}}$, since as for the $k = 0$ mode the imaginary part of the $k = N_{\mathrm{F}}$ Fourier mode also equals 0 for real functions. The structure of matrix A is the following:

$$A = [A_1\, A_2\, \cdots\, A_S],$$

where the A_s are $N \times (N_s + 1)$ matrices such that $[A_s]_{ki} = \hat{L}^s_{i,k}$.

3. Comments and preliminary numerical results

- If for any $s, N_s + 1 \leqslant N^s_{\mathrm{F}}$ and if $N < N_{\mathrm{F}}$, then functions only differing from their highest Fourier modes, say $f^1(x), f^s(x), \ldots$ such that $\hat{f}^1_k = \hat{f}^2_k = \cdots$ if $k \leqslant N$, yield the same piecewise polynomial interpolant $g(x)$.
- If $N_s + 1 = N^s_{\mathrm{F}}$ for any s, so that $N = N_{\mathrm{F}}$, in each interval $[y_{s-1}, y_s[$ we simply get the polynomial interpolant of the set $\{f(x_j), x_j \in [y_{s-1}, y_s[\}$. But as it is well known, for nonsmall values of N_s such a polynomial interpolant may show large oscillations between the grid-points, especially when they are equidistant. Note that with the above assumptions matrix A is regular: For a given set $\{f(x_j)\}_{j=1}^{N_{\mathrm{F}}}$ there exists one and only one piecewise polynomial interpolant.
- Matrix A is regular if and only if $N_s + 1 \leqslant N^s_{\mathrm{F}}$, $1 \leqslant s \leqslant S$. Let us assume $N_s + 1 \leqslant N^s_{\mathrm{F}}$ and consider Eq. (5) for all the Fourier modes. Because the $L^s_i(x)$ are linearly independent and completely defined by their values at the N_{F} Fourier points, the resulting system is of maximum rank, i.e., of rank N. Removing the highest Fourier modes ($k > N$) preserves the rank, so that A is of rank N and thus regular. Assume now that for a particular s, $N_s + 1 > N^s_{\mathrm{F}}$. Then one can build a non-null polynomial of degree N_s, say $u_s(x)$, such that $u_s(x_j) = 0$ if $x_j \in [y_{s-1}, y_s[$. The solution to the initial problem is thus not unique and consequently matrix A is in this case singular.

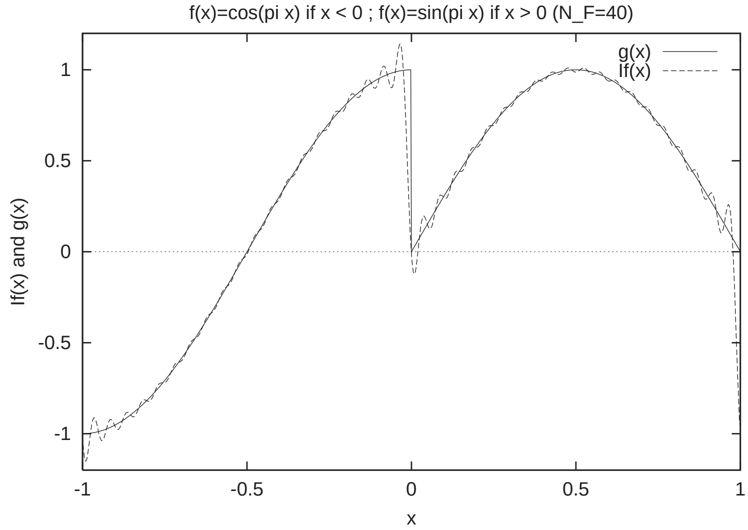

Fig. 1. Trigonometric interpolant of $f(x)$ and reconstructed function $g(x)$.

Remark. In the continuous framework matrix A is regular. However, if a quadrature rule is used to compute the integrals, as a result of the present analysis the number of quadrature points in each interval must be greater than (or equal to) $N_s + 1$.

- One can state the following convergence property: If in each interval $[y_{s-1}, y_s[$ the restriction of $f(x)$ is C^∞ (f and all its derivatives are continuous), then the inverse reconstruction method is spectrally accurate. This directly results from the fact that since it is exact for polynomials one recovers for each interval all the properties of spectral methods based on orthogonal polynomials. This convergence result is visualized in Fig. 1 where we compare the trigonometric interpolant, say $\mathscr{I}f$, of $f : [-1, 1[\to \mathbb{R}$ such that

  $$f(x) = \cos(\pi x) \quad \text{if } x < 0, \qquad f(x) = \sin(\pi x) \quad \text{if } x \geqslant 0$$

  with the reconstructed function $g(x)$ for $N = N_{\mathrm{F}} = 40$.
  The error, in the max-norm (discrete L^∞ norm), between the exact and the reconstructed solution is plotted in Fig. 2. One clearly observes an exponential decay, at least till a critical value $N_{\mathrm{F}} \approx 40$. Beyond $N_{\mathrm{F}} \approx 40$ the error is nolonger decreasing but increasing, which is meaningful of the fact that the condition number of matrix A deteriorates when N_{F} is increased, i.e., that the stability property required for a system to be well-posed is not fulfilled.
- If $N = N_{\mathrm{F}}$, an exponential increase of the condition number of matrix A is indeed observed in Fig. 3, where the reciprocal condition number of A is plotted. Different Gegenbauer polynomial bases (including the Legendre's), i.e., different values of the parameter λ appearing in the Gegenbauer weight $(1 - x^2)^{\lambda - 0.5}$, have been used in order to numerically check that for inverse methods changing the polynomial basis offers no interest. These results have been obtained by using a partition of $[-1, 1[$ in the two subintervals $[-1, 0[$ and $[0, 1[$.

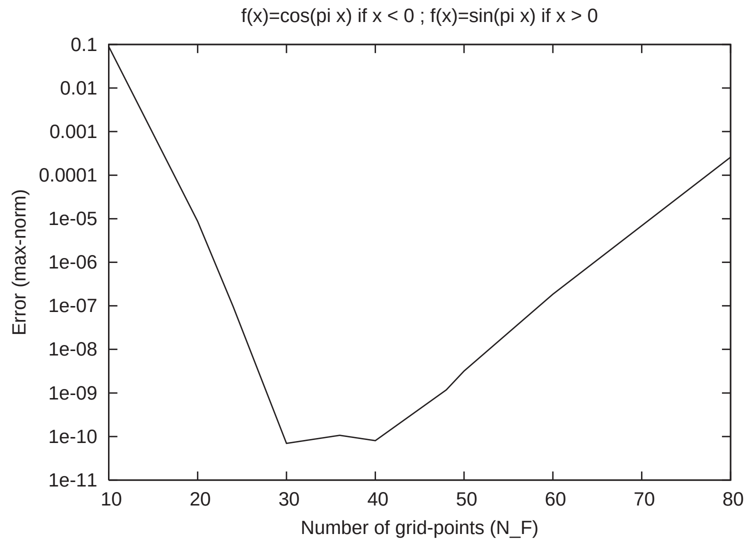

Fig. 2. Error between the exact and the reconstructed function vs. the grid-point number N_F.

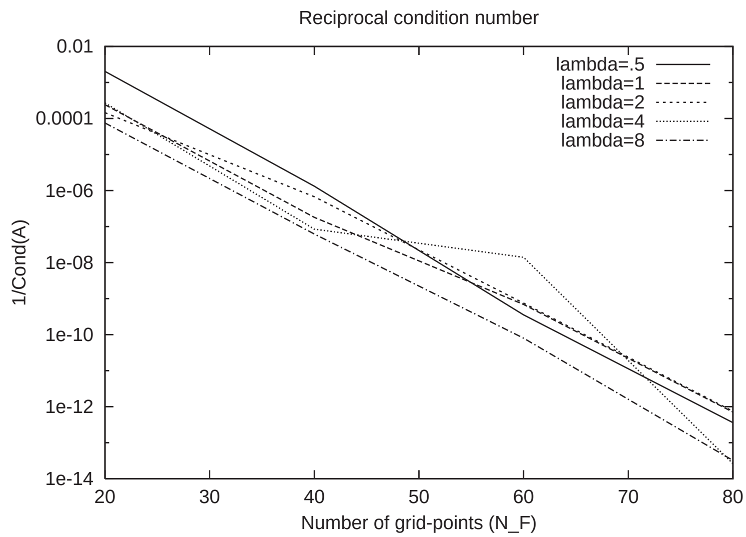

Fig. 3. Reciprocal condition number of the matrix A for different Gegenbauer bases (Legendre basis for $\lambda = 0.5$).

- As shown in Fig. 4, where the reciprocal condition number of matrix A is plotted for different values of the ratio $\sigma = N_F/N$ $(= N_F^s/(N_s + 1)$, for any $s)$, if $N < N_F$ the increase of the condition number is slower but remains exponential. Moreover, for $\sigma \geqslant 2$ one observes a saturation effect. From this result it is clear that in the limit $\sigma = \infty$, corresponding to the continuous case investigated in [11], the inverse problem is similarly ill-posed.

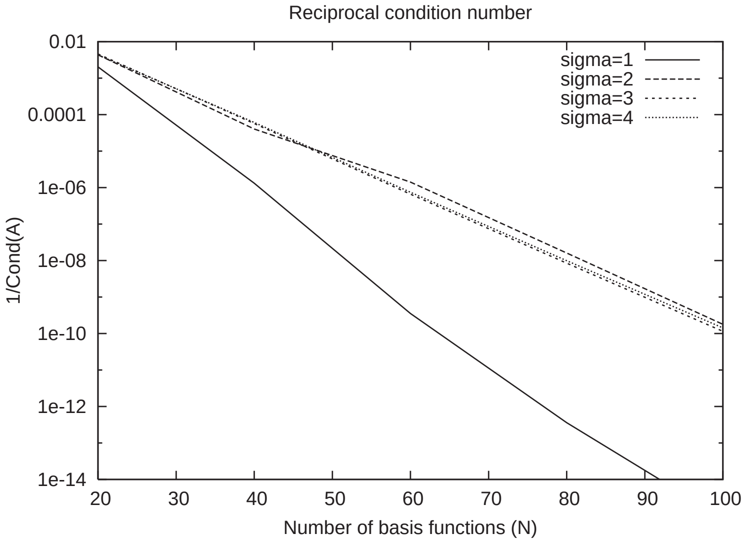

Fig. 4. Reciprocal condition number of the matrix A for different values of σ ($\lambda = 0.5$).

4. Capabilities and limits of inverse methods

Here we first show some attractive results that can be obtained with the inverse discrete method. We consider in fact two versions of the method, that we call global or local. By increasing the parameter σ and/or by going to the local version of the method one can by-pass, at least for the polynomial degree values used in practice, the ill-posed feature of the inverse problem. Note that the natural way to overcome the stability problem when N becomes large is of course preconditioning, i.e., to solve $CA\tilde{\boldsymbol{g}} = C\hat{\boldsymbol{f}}$, where C is an approximate inverse of A in such a way that the matrix CA shows a O(1) condition number. However such a task is not trivial, as pointed out by the complexity of the Gegenbauer polynomials based direct method, in contrast with the simplicity of the inverse approach. It is indeed clear that a preconditioner resulting from the direct approach would be a good preconditioner.

4.1. Capabilities

To demonstrate numerically the efficiency of an increase of σ, let us consider the following function $f : [-1, 1[\to \mathbb{R}$, discontinuous at $x = 0$:

$$f(x) = -\cos(7.5\pi x) \quad \text{if } x < 0, \qquad f(x) = \cos(7.5\pi x) \quad \text{if } x \geqslant 0. \tag{6}$$

Of course, such a function is more oscillating than the one considered in Section 3, so that a satisfactory reconstruction requires a greater number of polynomials. In Fig. 5 we compare the decrease of the error when using $\sigma = 1$, 2 and 4. Clearly, with $\sigma = 1$ the method fails due to the stability problem whereas more satisfactory results can be obtained for $\sigma \geqslant 2$.

As in [4] , the basic idea of the local method is the following: For x "close" to the discontinuity points one uses the inverse method and elsewhere a standard filtering, so that only small values of

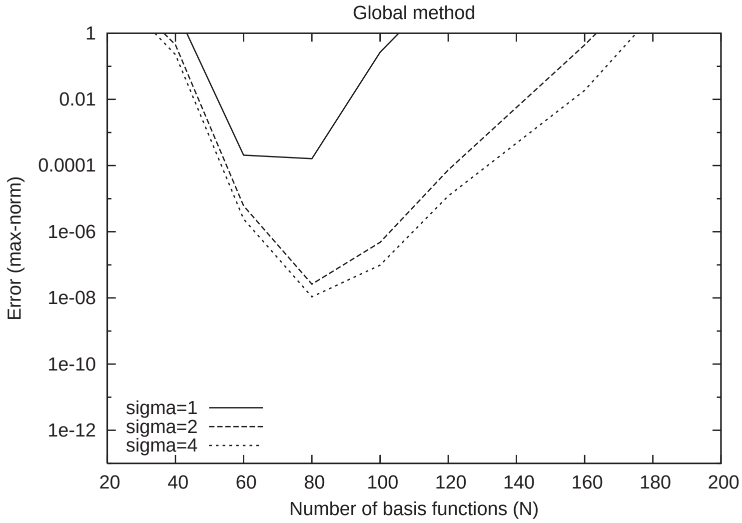

Fig. 5. Global method: error vs. N for different values of σ.

N are considered. Thus, let us assume that $f(x)$ is not continuous at $x = Y$ and smooth everywhere else. Then we can apply the (global) inverse method only in an interval $(Y - \delta Y, Y + \delta Y)$, and some standard filtering elsewhere, by simply disregarding the result of the filtering procedure in $(Y - \delta Y, Y + \delta Y)$. More precisely, one may select the grid-points $x_{i_1} \approx Y - \delta Y$ and $x_{i_2} \approx Y + \delta Y$ and build a P-periodic function $h(X)$, where $X = P(x - x_{i_1})/(x_{i_2} - x_{i_1})$, as the trigonometric interpolant defined from the set $\{f(x_i)\}_{i_1 \leqslant i < i_2}$. Then, one applies the global reconstruction procedure to $h(X)$ and combine it with the filtering technique out of the interval $[x_{i_1}, x_{i_2}[$.

The results obtained for the test-case (6), with $\delta Y = 0.5$ and using the "raised cosine filter" (see e.g. [3]), are presented in Fig. 6. One observes that due to the fact that a large polynomial degree is useless in the smaller intervals that are considered, the stability problem is less sensitive. However, out of the interval $[-0.5, 0.5[$, the error is of course much greater, as shown in Fig. 7. To visualize the efficiency of the hybrid technique the oscillating Fourier interpolant obtained for $N = 30$, $\sigma = 1$, $\delta Y = 0.5$ and the reconstructed function are shown in Fig. 8.

Remark. The advantage of the local method described here is to open a way toward multi-dimensional complex geometries. Especially, extending the 1D ($d = 1$) global inverse method to the 2D or 3D problems is a priori difficult: (i) Except for specific situations, for which the lines ($d = 2$)/surfaces ($d = 3$) of discontinuities define Cartesian geometries, the reconstruction procedure must be carried out for surfaces/volumes of complex shape; (ii) Assuming that N basis functions are used in each direction, the size of the (full) system matrix A equals $N^d \times N^d$, which is by far too large. The coupling of standard filtering with the local method appears much more realistic, the local reconstruction procedure being only carried out in zones including the discontinuity lines/surfaces. A similar approach is besides the one used for the direct reconstruction method, see e.g. [1,5], which however also suffers of point (i).

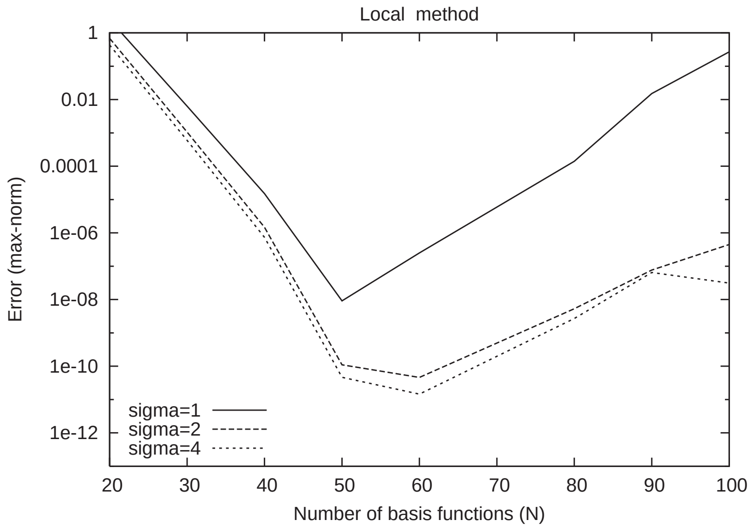

Fig. 6. Local method (reconstructed part): error vs. N for different values of σ.

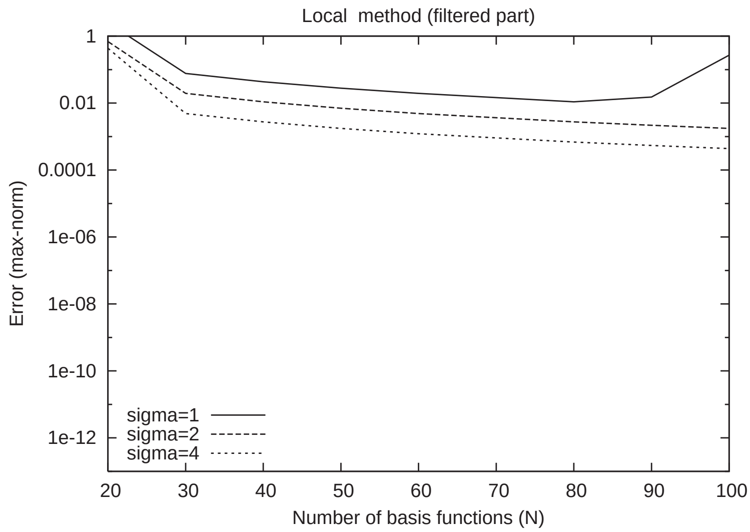

Fig. 7. Local method (filtered part): error vs. N for different values of σ.

4.2. Limits

We have just shown how inverse methods can achieve accurate reconstructions of discontinuous functions from their Fourier spectra. However, it should be observed that in all the examples that we have considered there was no grid-point to grid-point oscillations, as generally induced by the Gibbs phenomenon. In all these examples it is the polynomial interpolant which is oscillating: linear

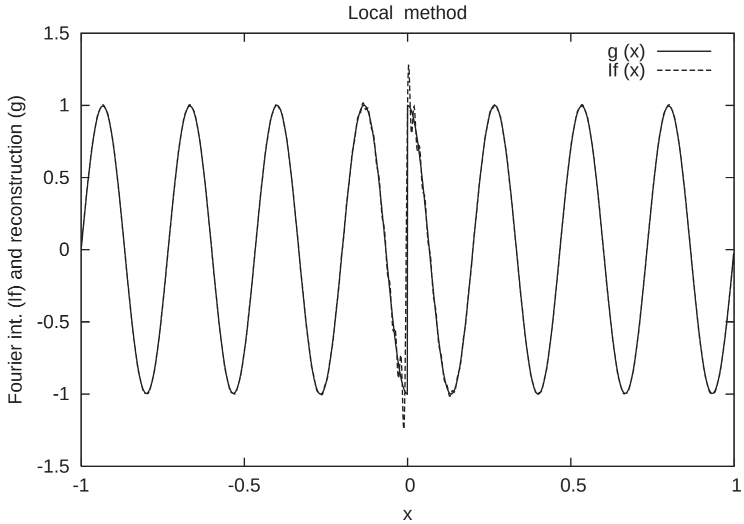

Fig. 8. Trigonometric interpolant of $f(x)$ and reconstructed function $g(x)$ ($\sigma = 2$) in $(-0.5, 0.5)$ and filtering elsewhere.

interpolations between the $f(x_j)$ would not show any oscillatory behavior. We are going to point out that the case of grid-point to grid-point oscillatory behavior may be more difficult.

To this end let us consider the rather simple function $f : [-1, 1[\to \mathbb{R}$ such that

$$f(x) = 1 + x \quad x < 0, \qquad f(x) = -1 + x \quad \text{if } x \geqslant 0. \tag{7}$$

Given a set of N_F Fourier grid-points $\{x_j\}$ and the corresponding $f(x_j)$, we can obtain an exact reconstruction. Note that this is even possible for $N = N_F = 4$, since the two polynomial interpolants are of degree 1! However the trigonometric-interpolant:

$$f_{N_F}(x) = \sum_{k=-N_F/2}^{N_F/2-1} \hat{f}_k \exp(\mathrm{i}k\pi x)$$

is of course oscillating.

To obtain a point to point oscillating behavior one can use a phase-lagging effect. Thus, the set of N_F values $\{f_{N_F}(x_j + \delta x/4\}$, where δx is the grid-step size, is strongly oscillating. Such a set of oscillating values can be simply obtained:

(i) From the $f(x_j)$ compute the $\hat{f}_k$,
(ii) compute the $\hat{f}'_k$ such that $\hat{f}'_k = \hat{f}_k \exp(\mathrm{i}k\pi\delta x/4)$,
(iii) compute by IFT (Inverse Fourier Transform) the $f'(x_j)$.

The functions $f(x)$ and $f'(x)$ are compared in Fig. 9, using linear interpolation between the grid-points. As desired the $f'(x_j)$ values are affected by strong oscillations.

The result obtained with the global and local methods are given in Fig. 10 and Fig. 11, respectively. Clearly both methods fail here to give a satisfactory result. Even more, a standard filtering would have been more efficient, as may be noticed in Fig. 11, where out of the interval $(-0.5, 0.5)$ it is

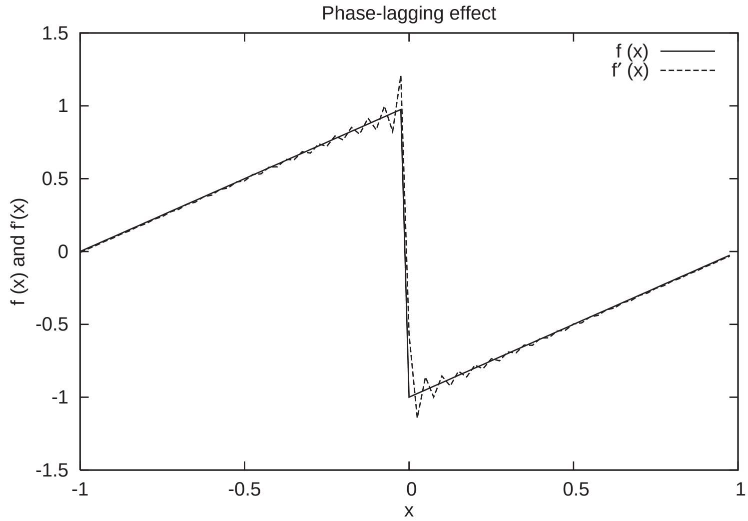

Fig. 9. The $f(x)$ and $f'(x)$ functions ($N_F = 80$).

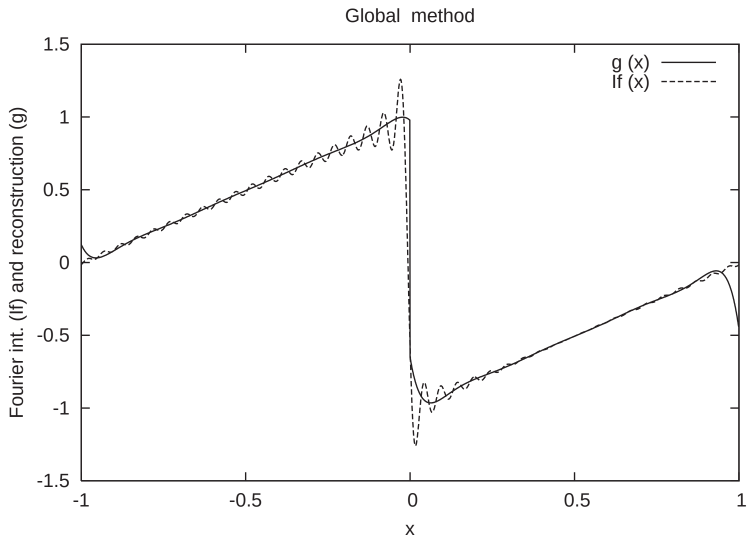

Fig. 10. Trigonometric interpolant of $f'(x)$ and reconstructed function $g(x)$ using the global method ($\sigma = 4$). In the interval $[-1, 0[$ and $[0, 1[$ polynomials of degree 9 are used.

the standard "raised cosine filter" which is active. Such a test-case clearly shows the limits of the proposed inverse reconstruction methods, even if for the considered example one may argue that it is in fact the discontinuity point abscissa which is approximative and that an edge detection procedure, as e.g. developed in [5,6], is here necessary.

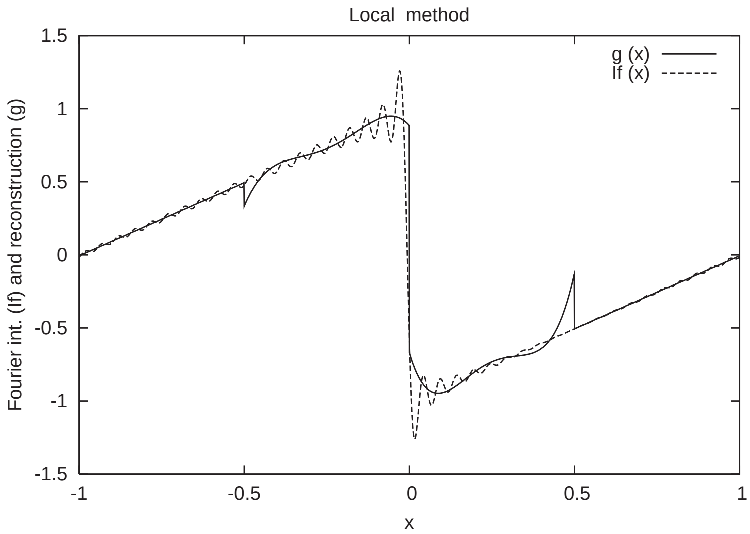

Fig. 11. Trigonometric interpolant of $f'(x)$ and reconstructed function $g(x)$ using the local reconstruction ($\sigma = 4$) in $(-0.5, 0.5)$ and filtering elsewhere. In the intervals $[-0.5, 0[$ and $[0, 0.5[$ polynomials of degree 4 are used.

5. Conclusion

The aim of this paper was to develop inverse discrete methods for the reconstruction of non-smooth periodic functions from their Fourier spectra. The main difficulty of such inverse approaches comes from the ill-posed feature of the corresponding inverse problems. It has been pointed out that this difficulty could be partially overcome by using piecewise polynomial approximations of degree twice smaller than the number of Fourier-grid points in the corresponding interval. The study has been carried out for global and local reconstruction methods. For the latter, which is a priori better adapted to handle multidimensional problems, we have shown how to combine standard filtering with local reconstruction. These discrete inverse reconstruction methods have been developed for Fourier approximations of periodic functions. However they can a priori be trivially applied to other spectral approximations, by substituting standard polynomial bases, like the Legendre or Chebyshev ones, to the Fourier basis. Finally, both the capabilities and limits of these inverse methods have been clearly emphasized.

Acknowledgements

We thank B.D. Shizgal and J.H. Jung, from the University of British Columbia, for stimulating discussions.

References

[1] R. Archibald, A. Gelb, Reducing the effects of noise in image reconstruction, J. Sci. Comput. 17 (1–4) (2002) 167–180.
[2] J.P. Boyd, Chebyshev and Fourier Spectral Methods, 2nd Revision, Dover Publications, New York, 2001.
[3] C. Canuto, M.Y. Hussaini, A. Quarteroni, T.A. Zang, Spectral Methods in Fluid Dynamics, Series in Computational Physics, Springer, Berlin, 1988.
[4] A. Gelb, A hybrid approach to spectral reconstruction of piecewise smooth functions, J. Sci. Comput. 15 (3) (2000) 293–322.
[5] A. Gelb, E. Tadmor, Detection of edges in spectral data, Appl. Comput. Harmon. Anal. 7 (1) (1999) 101–135.
[6] A. Gelb, E. Tadmor, Detection of edges in spectral data. II: nonlinear enhancement, SIAM J. Numer. Anal. 38 (4) (2000) 1389–1408.
[7] D. Gottlieb, C.-W. Shu, On the Gibbs phenomenon and its resolution, SIAM Rev. 39 (4) (1997) 644–668.
[8] D. Gottlieb, C.-W. Shu, A. Solomonoff, H. Vandeven, On the Gibbs phenomenon 1: recovering exponential accuracy from the Fourier partial sum of a nonperiodic analytic function, J. Comput. Appl. Math. 43 (1992) 81–92.
[9] D. Gotttlieb, J.S. Hesthaven, Spectral methods for hyperbolic problems, J. Comput. Appl. Math. 128 (2001) 83–131.
[10] R. Peyret, Spectral methods for incompressible viscous flow, Applied Mathematical Sciences, Springer, Berlin, 2002.
[11] B.D. Shizgal, J.-H. Jung, Towards the resolution of the Gibbs phenomena, J. Comput. Appl. Math. 161 (2003) 41–65.